Influence of Aging Heat Treatment on Pitting Corrosion Resistance of Martensitic Stainless Steel

Abdullah Dhayea Assi

Middle Technical University/Institute of Technology- Baghdad/Baghdad/Iraq
Email: drabdullah_dhayea@mtu.edu.iq

Abstract

This research aim to study the influence of aging heat treatment on the pitting corrosion resistance of martensitic stainless steel (MSS), where a number of martensitic stainless steel specimens were subjected to solution treatment at 1100 ºC for one hour followed by water quenching then aging in the temperatures range (500-750) ºC for different holding times (1, 5, 10, 15 & 20) hr. Accelerated chemical corrosion test and immersion chemical corrosion test were performed on samples after heat treatment. The results of the research showed that the pitting corrosion resistance is significantly affected by the aging temperature. where samples that aged at 500 °C have the highest rate of corrosion due to an increase in the ratio of the Delta ferrite (δ-ferrite) and very soft precipitates from other phases of heterogeneous form in the basic martensitic phase; which leads to increase corrosion rate. From the other side, the aged samples in the temperature range (550–650) °C have the smaller rate of corrosion, this is due to the high volumetric ratio of remaining austenite. The aged samples at temperatures above 650 °C shows a medium corrosion rate. It was also found that the type of pits results from both the chemical corrosion tests and their shape were not related to the ferrite type and the carbides present in the microstructure.

Keywords: Martensitic, Stainless Steel, thermal aging, pitting corrosion resistance.

1. Introduction

The need to use steels at medium operating temperatures and high ratios of tensile strength to the weight led to develop one type of stainless steel which have corrosion resistance and hardened by precipitation, the martensitic type. These types of stainless steel have proven their efficiency in applications with chemical corrosion resistance, such as oil, marine and nuclear applications, as they are exposed to corrosive media. The chemical corrosion resistivity of martensitic stainless steel which has corrosion resistance and hardened by precipitation is better than other martensitic types and can be compared with austenitic stainless steels in most media. Therefore, it widely used in military and non-military equipment, and completely preferred compared with immersed and refractory martensitic steels [1].

Electrochemical studies of chemical corrosion of stainless steel have shown that the chemical composition and microstructure of these steels are important factors in determining chemical corrosion behavior. As well as, the chromium content of stainless steel is important in order to obtain and maintain good chemical corrosion resistance under certain operating conditions. If the chromium content is low at the granule boundary, the steel will be vulnerable to attack and corrosion among the granules even if there is high chromium content in the basic freezing solution. On the other side, if chromium-rich carbides are concentrated on the grain boundaries, there will be a shortage of chromium in the vicinity of the boundary and the carbides

will begin to settle there. This will corrupt the chemical corrosion resistance in these areas and will result in granule local corrosion [2].

The study of the chemical wear behavior of stainless steel that can be quickly deposited and frozen shows that it is produced in the form of chrome-rich and molybdenum-rich carbide on the boundary of grains, which can be the cause of the high susceptibility of these alloys to pitting corrosion [3].

The heat treatment of stainless steels helps to produce changes in the physical state, mechanical properties, residual stress levels, and in restoring maximum chemical corrosion resistance when these properties are adversely affected by various manufacturing or heating processes. An acceptable combination of resistance to chemical corrosion with optimum mechanical properties can be obtained by appropriate choice of heat treatment. In general, any improvement in the mechanical properties of steels by rapid cooling and revision will inevitably associated with increased chemical corrosion [4].

The general corrosion behavior of sintered 17-4 PH stainless steel processed under different processing conditions in dilute sulfuric acid solution at 25 °C was studied by open-circuit potential measurement and potentiodynamic polarization technique. The results showed that the precipitation-hardening treatment could significantly improve the corrosion resistance of the sintered 17-4 PH stainless steel in studied environment. It can be concluded that the highest corrosion resistance in 0.5 M H2SO4 solution exhibits 17-4 PH after solution treatment at 1040 °C followed by aging at 480 °C [5].

Pitting corrosion properties were investigated in 0.6M NaCl electrolyte with sulfate additions by

Potentiodynamic Polarization (PP). Hardness, tensile and yield strength of the UNS S46500 steel after lower aging temperature, 510ºC (H950), are higher than the ones found in the 538ºC (H1000) aged steel. This result is explained by microstructure, X-ray diffraction and Thermo-Calc analysis, which indicated the presence of austenite, chi phase and probably Ni3Ti precipitates finely and uniform distributed throughout the martensite matrix [6].

The aim of this research is to study the influences of aging heat treatment and the resultant phases on the pitting corrosion resistance of martensitic stainless steel through accelerated chemical corrosion as well as immersion chemical corrosion tests that have to be performed on samples after aging heat treatment. This is due to the necessary need for this type of stainless steel in various applications.

2. Experimental Work
2.1. Materials

The materials used in this research are martensitic stainless steel sheets hardened by precipitation hardening that was pre-exposed by the manufacturer to the normalizing process at a temperature of 924 °C, then cooled in the air and exposed to aging process at 600 °C. It finally cooled in the air to room temperature. The chemical analysis of the used steel was obtained by the spectroscopy device (Model Spector Max-X). Table (1) shows the chemical composition of this steel and Steel grade 420SS [7].

Table 1,
The chemical composition of the used stainless-steel.

Element %	C	Cr	Ni	Mo	Si	Mn	S	P	Ti	Fe
Standard [7]	0.07	15-17	3-5	0.5-2	0.25-0.5	0.5-1	0.002	0.01-0.04	0.45	Bal.
Measured	0.05	15.5	5.6	0.80	0.3	0.70	0.002	0.02	0.4	Bal.

2.2. Heat Treatment

The previous sheets were cut into 32 samples with dimensions of (10 × 5 mm) for each sample, and then subjected to the following heat treatments:
1- Solution treatment at 1100 °C for one hour, then immersed in water.

2- Aging at temperatures 500, 550, 600, 650, 700, and 750 °C for five hours, and then cooled by air
3- Aging at two temperatures 500 and 650 °C during different times 1, 5, 10, 15, and 20 hours.
The samples were heated using two electric furnaces as shown in Figure (1a), the first for the dissolution treatment and the second for the aging process .

Fig. 1a. Two Electric Furnaces for heat treatment.

2.3. Chemical Corrosion Test (dynamic voltage or acceleration test)

Chemical corrosion testing or acceleration testing is an effective widely used method in estimating the chemical corrosion in aqueous media by passing a current into the electrode using an inert electrode. The degree of polarization is determined by measuring the sample voltage, while the rate of electrode reaction is measured from the density of the cell current that it directly transits to a chemical corrosion rate measured in mm/year. The anode and cathode polarization diagrams of electrodes (samples) exposed to a 6% $FeCl_3$ solution are plotted and the electrode area is 0.5 cm^2. These diagrams are obtained using PS6 device connected with a computer. The voltage range was found in all tests from - 200 to +1000 mV, and the scan rate was set to 0.5 mV/s. This test was carried out

at room temperature at the Ministry of Science and Technology / Department of Materials as shown in Figure (1b).

Fig. 1b. The Chemical Corrosion Test.

2.4. Pitting Chemical Corrosion Test (Immersion Test)

The pitting chemical corrosion resistance was measured according to ASTM G48 for pitting test by using a ferric chloride ($FeCl_3$) as immersion solution with a concentration of 6% prepared by dissolving 100 g of aqueous ferric chloride ($FeCl_3$. $6H_2O$) in 900 ml distilled water.

The test was carried out in the following manner:

1- The samples are firstly weighed

2- The samples are immersed in the previous solution for 72 hours.

3- The samples are removed from the solution and washed with distilled water to remove dissolved oxides that have formed on the surface of the samples,

4- The samples are weighed again.

5- The weight loss is calculated by the difference between the two weights.

Finally, the samples are examined under a microscope at 50 times magnification and the pitting spots formed on the surface of the samples are captured according to the previous specification with changing the immersion solution after each immersion and existing process of samples.The corrosion rate can be calculated by equation (1) [Reference]:

Where: $$CR = \frac{3650 \times W}{A \times d \times t} \qquad \ldots(1)$$

CR: Corrosion rate (mm / year)

W: Weight loss = Initial Weight - Final Weight in (grams)

A: Sample exposed surface area (cm^2)

d: Tested material density (gm / cm^3)
t: Immersion time (day)

2.5. Microstructure Test

The microstructures of the heat-treated samples that were subjected to chemical corrosion tests have been examined by using an OLYMPOS optical microscope. Samples were prepared for microscopic examination of sharpening, polishing and smoothing with Fry solution for smoothing consisting of (5g from CuCl$_2$ copper chloride) + (40 mL from HCl) + (30 mL from methyl alcohol) and 30 mL of water. The phases and microscopic components, such as the martensitic matrix and the Delta ferrite phase, were identified using an optical microscope, since the martensitic floor appeared in the form of plates, while the Delta type ferrite appeared in small quantities in the form of longitudinal white ribs, and no presence of austenite was found in this sample, as indicated by in Figure (2).

The volumetric ratios for the Austenite were determined using XRD diffraction technique according to the method described in ASTM E975-95.
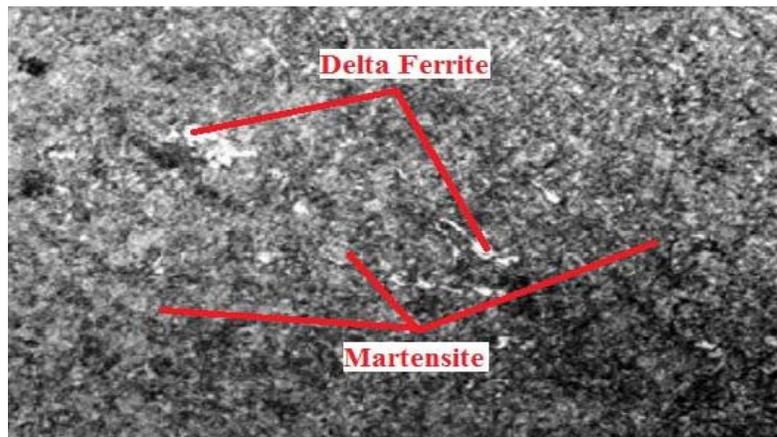
Fig. 2. The microstructure of soluble treated samples at a temperature of 1100 °C (50X).

3. Results
3.1 Effect of aging process on austenite volumetric ratios

Figure (3) shows the effect of aging temperature on the austenite volumetric percentages. It was found that by increasing the aging temperature, the austenite volumetric ratios gradually increase, and the maximum value of the austenite volumetric ratios occurs at a temperature of 650 °C. After that, a gradual decrease was occurred down to temperature of 750 °C.
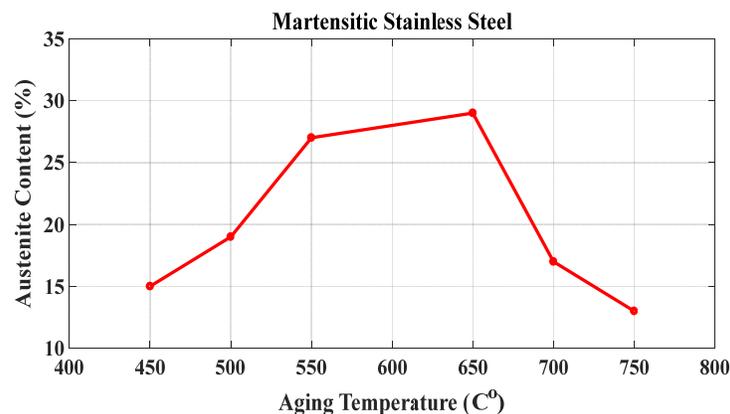
Fig. 3. Effect of four hours aging temperature on volumetric ratio for austenite.

The effect of aging time on the austenite volumetric percentages at 500 and 650 ° C aging is shown in figure (4). No significant change in the residual austenite volumetric percentages at 500 °C was noticed. While at aging temperature of 650 °C increases the amount of austenite was significantly increased from 20% to 55%; by increasing the aging time from 1 to 20 hours.

Martensitic Stainless Steel
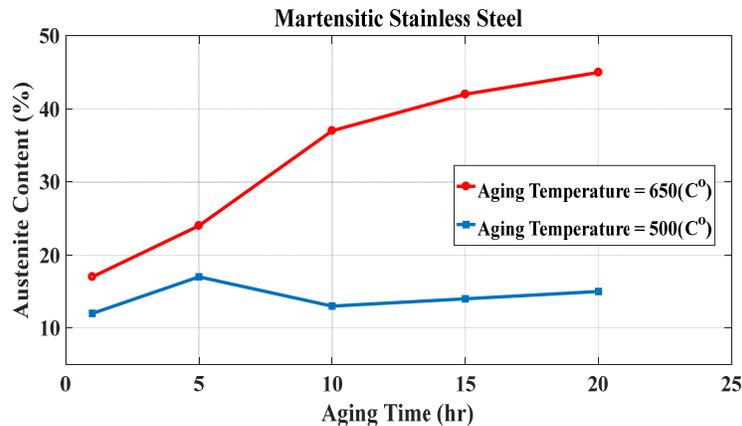
Fig. 4. Effect of aging time on the austenite volumetric percentage at two aging temperatures.

3.2 The Effect of Aging Process on the Microstructure

The microscopic structure of heat-treated samples at different aging temperatures and times were shown in Figures (5 to 11). All microscopic structures consist mainly of low carbon martensitic and variable percentages of ferrite delta type, which sometimes present in the form of Longitudinal ribs. The fundamental change in the microscopic structure with increasing aging temperature and time was the decomposition of martensitic associated with the appearance of austenite. The volumetric ratio of the austenite was increased by increasing the aging temperature up to 650 °C.

The microstructure of the aging samples at a temperature of 500 °C and a time of 4 hours was shown in Figure (5). The form of elongated carrots, Martensitic slices and also austenitic elongated granules, which arise between the Martensitic slices within the former austenitic granules, leading to the variation of the microscopic structure.

Figure (6) shows the microscopic image of the aging specimens at 500 °C for one hour. The typical low-carbon slice martensitic structure is shown in the former austenitic granule. The transformation of martensitic to austenite becomes more pronounced by increasing the aging temperature and time. At temperature aging of 550 °C for 5 hours the same microstructure as shown in Figure (7) where a high number of

longitudinal grounded austenite were pronounced. This decomposition of martensitic becomes more pronounced at temperatures of (550 and 600 °C) as shown in Figures (7 and 8) below . In this case the austenite volumetric percentage was about 20% as shown from previous Figure (3).

After the aging temperature of 600 °C for 5 hours, the microstructure is almost identical to that of the previous 550 °C as shown in Figure (8), but the residual austenite volume increases to about 30%.
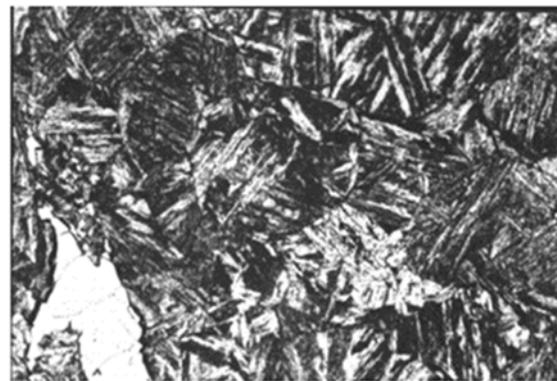
Fig. 5. **Microstructure of aging specimens at temperature 500 ° C and aging time 5 hrs 200 X.**
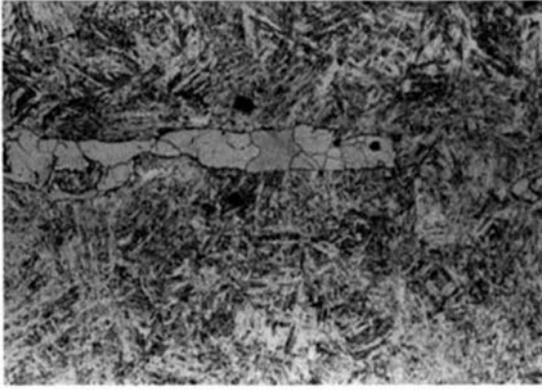
Fig. 6. Microstructure of aging samples at 550 ºC for 1 hour (200X).

Fig. 7. Microstructure of aging samples at a temperature of 550 oC for 5 hours (100X).

Fig. 8. Microstructure of aging samples at a temperature of 600 °C for 5 hours (200X).

The maximum residual austenite value of 32% is shown in the sample treated at 650 ° C for 5 hours as shown in Figure (9). The microstructure seems to be as equal axes granules, which can be seen inside these soft needle-shaped microstructures. Examination of this structure at

High magnification showed that the residual austenite granules are elongated, and their volumetric ratio increased with the aging time from 1 to 20 hours as shown in Figure (10). The former austenitic granules are dark in color and others are light in color and larger in size.
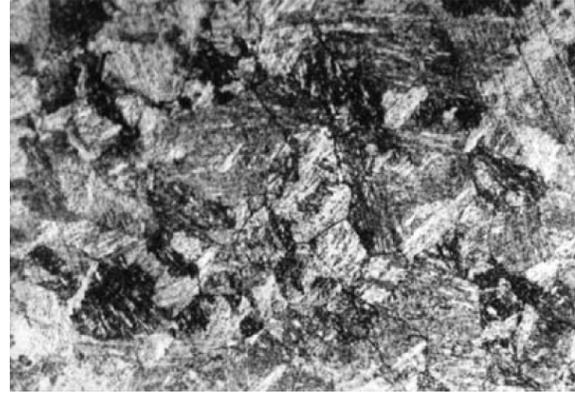
Fig. 9. Microstructure of aging samples at 650 ºC for 5 hours (200X).
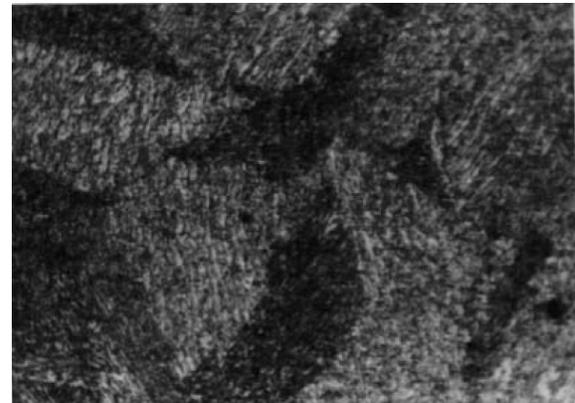
Fig. 10. Microstructure of aging samples at 650 ºC for 16 hours (1000X).

The microstructure of the aging samples at a temperature of 700 °C for 5 hours is shown in Figure (11). In this figure the ribs of ferrite delta type are shown and adjacent to them are often bright white elongated granules and others with almost equal axes. These granules are for the residual austenite which has been converted to non-aging martensitic.

25
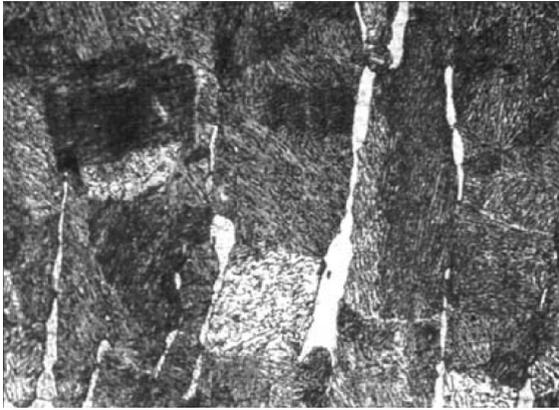
Fig. 11. Microstructure of aging samples at 700 ºC for 4 hours (500X)

3.3 Effect of aging process on chemical corrosion rate (dynamic voltage and immersion tests)

Figure (12) shows the effect of 5-hours aging temperatures on the chemical corrosion rate (with 6% iron chloride acceleration test) and immersion test, as it appears from this form the following points:

1. The chemical corrosion rate is increasing sharply in the aging temperature range from (500 to 550) °C.

2 - The largest value of the rate of chemical corrosion is about 2.5 mm / year; when aging to a temperature of 550 °C.

3. The chemical corrosion rate decreases steeply when aging in a temperature range of (550 to 600) °C

4 - The minimum value of the rate of chemical corrosion about 0.2 mm / year that produced at aging range of (550 to 650) °C.

5. The rate of chemical corrosion increases again, gradually, when aging after the previous field.
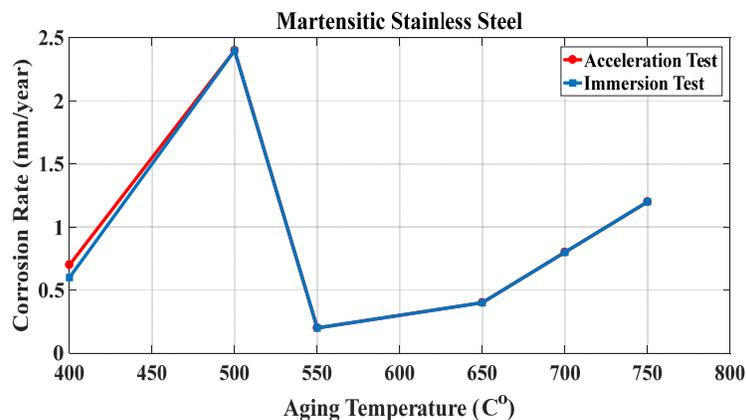
Fig. 12. Effect of 5-hour aging temperature on chemical corrosion rate due to acceleration test (dynamic voltage test) and immersion test.

Figure (13) shows the effect of aging time on the chemical corrosion rate; at 550 and 650 ° C aging temperatures, when aging at a temperature equal to 550 °C, the initial phase of chemical corrosion increases from 1 to 5 hours. The maximum value of the chemical corrosion rate was at an aging time of **5** hours, after which the rate of chemical corrosion gradually decreases. When aging at a temperature equal to 650 °C, the chemical corrosion rate gradually increases with the aging time and the increase rate is much faster after aging time of 10 hours.
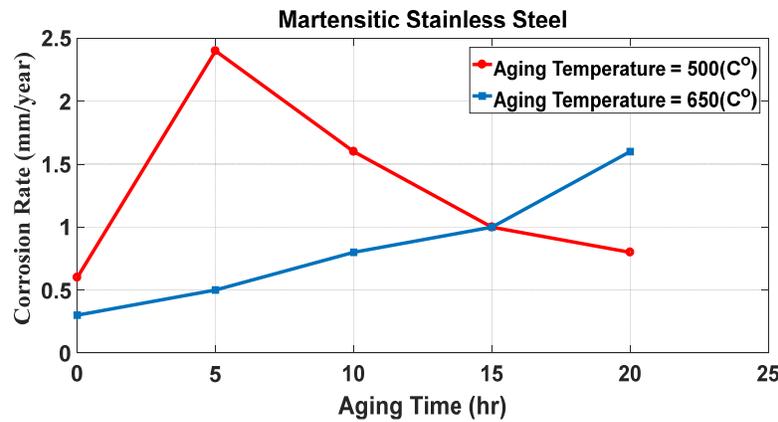
Fig. 13. Effect of aging time on the chemical corrosion rate of aging samples at an aging temperature of (500 and 650) °C from the accelerometer test (dynamic voltage test).

3.4 Effect of aging process on voltage

Figure (14) shows the effect of increasing the aging temperature on the voltage; at an aging time of 5 hours, this figure shows the following:
- The voltage decreases gradually by increasing the aging temperature in the range from (500 to 650) °C, and produces the lowest voltage when aging at 650 °C.
- The voltage increases significantly by increasing the temperature in the field from (650 to 750) °C.
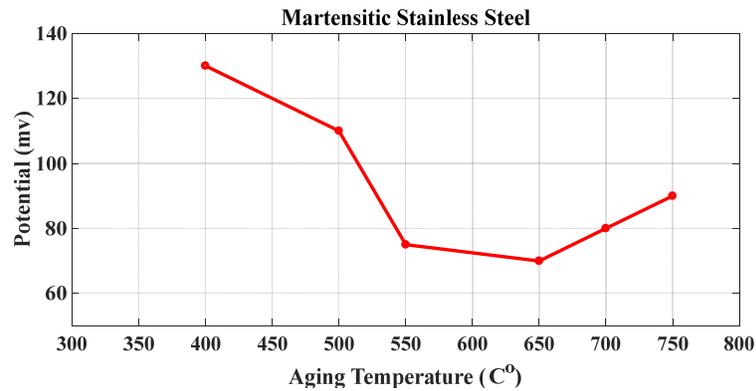
Fig. 14. Effect of aging temperature for 5 hours on voltage.

The effect of aging time on voltage is shown in Figure (15) at (500 and 650) °C. An increase in voltage is observed at each aging temperature, starting from an equal aging time to one hour, and the rate of increase is much faster at an aging temperature of 500 °C, and the maximum value of the voltage is produced by aging for 10 hours; this is at all the two temperature ranges of aging. On the other hand, the voltage decreases gradually when the aging time increases above 10 hours and after (15) hours the rate of decrease is slower. The aging sample at a temperature of 500 °C had a higher voltage than the aging sample at a temperature of
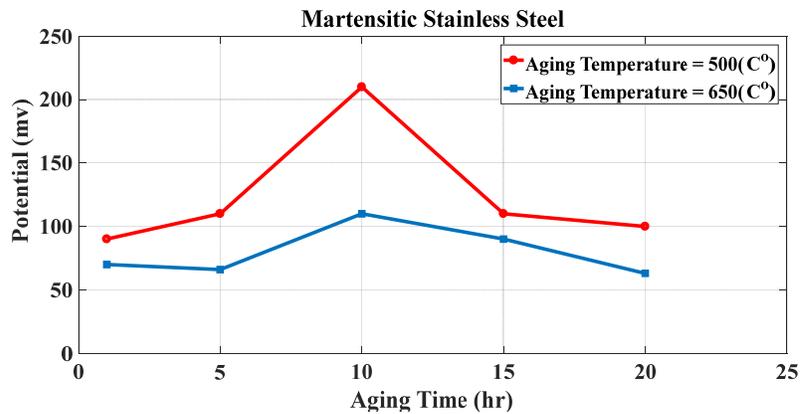
Fig. 15. Effect of aging time on voltage at two aging temperatures.

3.5 Effect of aging process on chemical corrosion rate (immersion test):

The changes in the chemical corrosion rate resulting from this test are shown in Figure (16). By changing the corrosion time of samples at the aging temperatures of (500 and 650) ° C, the changes in the rate of chemical corrosion by changing the aging time are similar to those resulting from the previous test (the accelerated test), but the values of the chemical corrosion rate are higher in this case.

The results can be studied and divided into two types:
1. The chemical corrosion rate of aging samples increases at 500 °C, in the first stage of the scheme from the time of aging 1 to 5 hours and the maximum value of the chemical corrosion rate occurs when aging for **5** hours, after which time the chemical corrosion rate gradually decreases with Increased aging time.
2. The rate of chemical corrosion gradually increases with the aging time of the aging samples at 650 °C, and the rate of increase is faster after aging time of 15 hours.
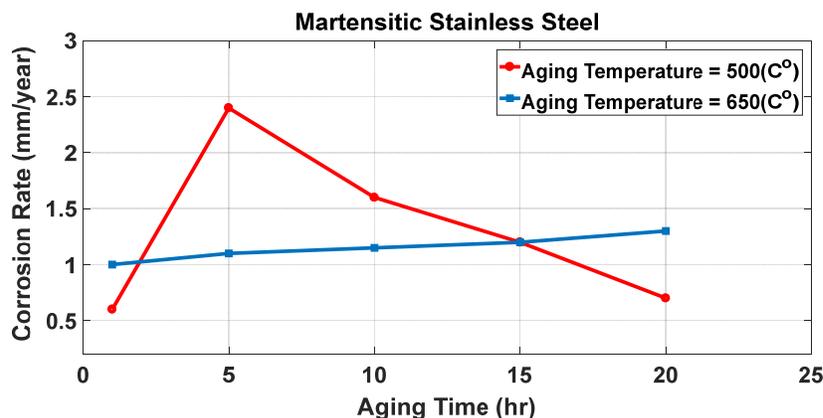
Fig. 16. Effect of aging time on chemical corrosion rate of aging samples at 500 and 650 °C aging temperatures.

3.6. Click forms in aging samples at different time temperatures

Figures (17) to (19) show microscopic images of aging samples at different aging temperatures and times tested by accelerated testing. From these images it can be seen that there is a deep and large mortise on the surface of the aging sample at a temperature of 550 ° C as shown in

Figure (17b), which corresponds to the high chemical corrosion rate previously measured.

When the sample is released at a temperature of 600 °C, the clicking is smaller and deeper than the rest of the sample as shown in Figure (17c), while the size of the tap formed on the surface of the aging sample at 750 °C is larger than that formed on the sample surface. The aging is 550

°C, but remains smaller than the aging sample at 500 °C, as shown in Figure (17f).

An increase in the aging time with the aging temperature constant at 500 °C indicates that there is a clear decrease in the flick size after being tested by acceleration method as shown in Figure (18), and the smallest flick size after aging is formed within a period of 20 hours as evident from Figure (18e). Conversely, by increasing the aging time at 650 ° C there is a noticeable increase in the size of the flick as shown in Figure (18), and the larger flick size is formed in the sample that was released at 20 hours as shown in Figure (18k).
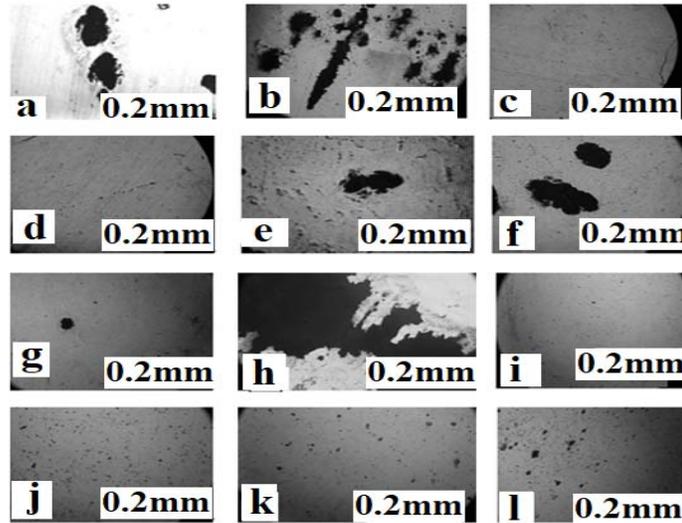
Fig. 17. Microscopic images of aging samples for 4 hours at different aging temperatures. (a, g) 500, (b, h) 550, (c, i) 600, (d, j) 650, (e, k) 700, (f, l) 750 °C, where (a, b, c, d, e, f, acceleration test) and (g, h, i, j, k, l, immersion test).
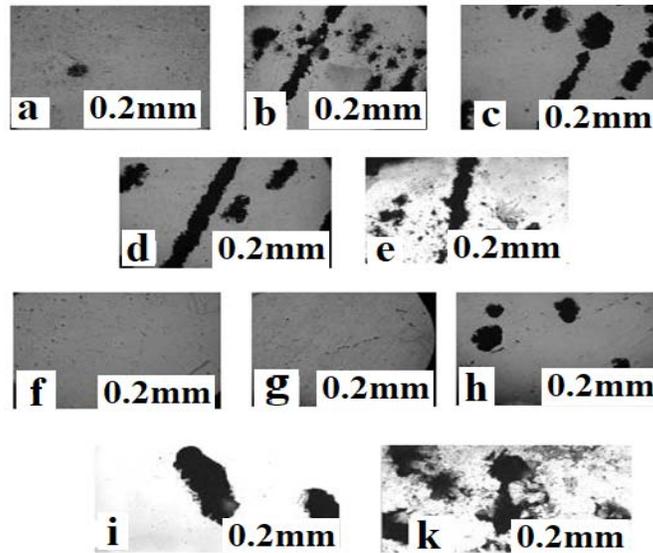
Fig. 18. Microscopic images of aging samples during different aging times;(a) 1hr, (b) 5hr, (c) 10hr, (d) 15hr, (e) 20hr: acceleration test where (a, b, c, d, e) at 500 °C and (f, g, h, i, k) at 650 °C.

Figure (19) shows the microscopic images of the aging samples at different temperatures and aging times. This is after being tested by immersion method, noting that there is almost no difference in the form of clicking and its size after aging at different temperatures and aging times; this is when compared to the pictures of the samples tested with the previously explained acceleration test as shown in Figure (18).
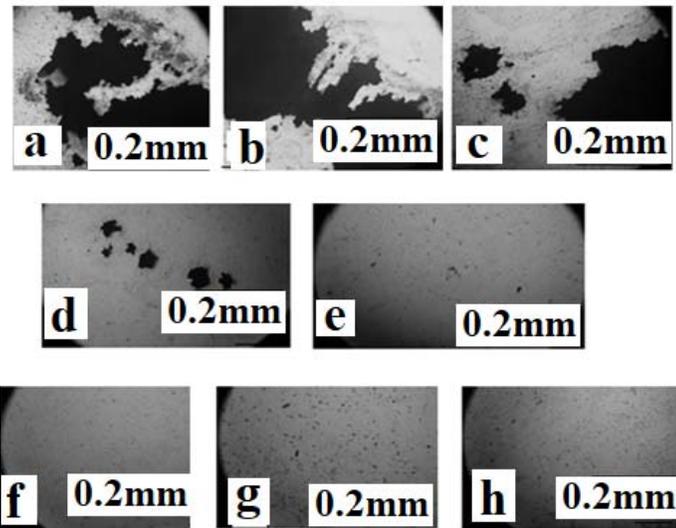
Fig. 19. Microscopic images of aging samples during different aging times ;(a) 1hr, (b) 5hr, (c) 10hr, (d) 15hr, (e) 20hr: immersion test where (a, b, c, d, e) at 500 °C and (f, g, h, i, k) at 650 °C.

4. Discuss the Results
4.1 The relationship between the aging process and the microstructure.

No residual austenite was observed in this type of stainless steel and rapidly cooled, probably because of the low residual austenite ratio of less than 2%; therefore, it did not appear in the microstructure and was not determined by X-ray diffraction.

The remaining austenite (quasi-slice austenite) may appear in areas where the returning austenite was formed after hemolytic treatment, so a double needle-shaped microscopic structure consisting of low-carbon martensitic and recovered austenite may be formed in each martensitic slice [8]. It is known that in some types of martensitic stainless steel can be converted to austenite after aging at an aging temperature equal to or above 500 ° C [9]. The remaining austenite ratios were found to increase with the aging temperature and time up to 650 ° C, as shown in Figures (3 and 4). It was also found that the amount of austenite was increased at the expense of martensitic by increasing the aging time above five hours at a temperature of 650 ° C; this means that the amount of martensitic converted to austenite remaining during the heating process at 650 ° C increased with the aging time.   The volumetric ratio of the austenite after aging process decreases at 700 °C or above compared to the aging process at a temperature range of 500-650 °C as shown in Figure (3); this means that the remaining part of

the austenite formed at these temperatures turned again into an aging martensitic. Aging at this temperature may have resulted in the deposition of chromium carbides $Cr_{23}C_6$ and titanium carbides (TiC) that consume carbon and depletion from martensitic and residual austenite [9]. This makes the austenite less stable and leads to the conversion of part of the remaining austenite to martensitic during cooling from 700 – 750°C to room temperature. After the rapid cooling process in the water, the microscopic structure of this sample consists of slices of martensitic and ferrite in the form of longitudinal ribs.

The formation of high-density slice martensitic in this hardened stainless steel can be justified by precipitation at high temperature starting temperature of the martensitic conversion of Ms = 120-150 °C as well as low carbon content in this steel, as it has been well proven that for various types of steels. The starting temperature of the martensitic transition and the ratio of carbon are the two most important factors that influence the structure and partial structure of Martensitic - and, in general, the martensitic with a slice structure is associated with a partial structure with a high intensity of dislocations [10]. It was found that aging samples were very deeply affected by the chemical smoothing solution as shown in Figures (5 to 11). This is due to the appearance of residual austenite among the martensitic segments .Exposure to the aging process at 500 ° C leads to a microscopic structure in which the martensitic bundles

dissipate or dissolve clearly. The residual austenite appearance and increased quantity between the martensitic slices up to a temperature of 650 ° C reduces the slide width from about 3 microns to 0.5 microns. The microscopic structure after aging at 700 °C for 5 hours appears to consist of equal-dimensional granules (axes) as shown in figure (11). This may be due to the different range of transitions from chilled martensitic to residual austenite and martensitic no aging, as well as carbides in different granules. These differences make the boundaries of the martensitic bundles can be resolved and dissipated.

4.2 The relationship between microstructure and chemical corrosion behavior

Chemical corrosion behavior has been affected by the aging time and its temperature, as well as by the amount of remaining austenite and ferrite type Delta, and also by the deposition of molybdenum and chromium carbides.

Aging-treated samples at 500 °C have maximum chemical corrosion rate values as shown in Figure (12). This could be due to the presence of delta-type ferrite in the form of longitudinal ribs and the deposition of very small precipitates found to be molybdenum carbides (Mo_2C) [11].

After aging for 15 hours at 500 ° C, these carbides may begin to disintegrate and this leads to a decrease in the rate of chemical corrosion as shown in Figures. (13 and16). Aging samples at 550 °C have the lowest corrosion rate values as shown in Figure (12), and this can be due to the high volumetric ratio of the austenite [12]. The resulting high rate of chemical corrosion after aging for 20 hours at 650 °C can be attributed to the beginning or growth of $Cr_{23}C_6$ chromium carbide. After aging at temperatures above 650 ° C, carbides of $Cr_{23}C_6$ type can become dominant, dominant and heterogeneous deposits in the martensitic floor that leads to an increase in the rate of chemical corrosion.

Aging in a range of (700 to 750) °C for 5 hours may precipitate $Cr_{23}C_6$ carbides at the grain boundary as chromium atoms leave to form chromium-rich carbides. If these chromium-rich carbides are concentrated on the grain boundaries, there will be a decrease in the chromium content in the vicinity where the carbides begin to settle, forming the depletion areas of the chromium. The grains became more dangerous in their resistance

to chemical corrosion [12]. The large flick size of aging samples at 500 °C as shown in Figures (17b), (18) and (19b) indicates that these samples are more susceptible to fovea corrosion, which may be due to the formation of molybdenum carbides and the presence of delta type ferrite. It can be concluded that aging samples at 500 ° C for 5 hours are less predisposition than other samples, due to the small click size as indicated by doubt (17c,i) and can be due to high volumetric percentages it remains the result of the dissolution and disintegration of martensitic. The formation of chromium carbides of type $Cr_{23}C_6$ in aging samples at 750 ° C has led to a second increase in the volume of clicking formed on the surface of aging samples at this temperature.

5. Conclusions

The main conclusions drawn from this research are the following:
1. The microscopic structure in rapidly cooled samples consists of slices of martensitic and longitudinal ribs of delta-ferrite and no residual austenite exists.
2. The remaining austenite begins to appear in the microstructure after aging at 500 ° C, and its volumetric ratios increase to its highest value after aging at 650 ° C.
3. The residual austenite volumes decrease from 32% to 20% by increasing the aging temperature from 650 to 750 °C. A portion of the remaining austenite is converted into an uncharacterized martensitic; this is cooled from 750 °C.
4. The chemical corrosion test was found to have three critical temperatures:
- High corrosion rate at 500 °C due to the presence of Delta -ferrite and Mo_2C carbides.
- Low corrosion rate at 500-650 ° C, due to high volumes of residual or anatomic.
- Average corrosion rate at 750 ° C as a result of deposition of chromium carbides and titanium in a small amount.
5. The aging temperature range from 500 to 650 ° C produced minimum localized corrosion that can be attributed to the high volumetric percentages of residual austenite.

6. References

[1] B. Tzaneva, "Effect Of pH on the Corrosion Behaviour Of High Nitrogen Stanless Steel in Chloride Medium," Journal of Chemical Technology and Metallurgy, 48, 4, 2013, pp 383390.

[2] R. C. Newman, "Understanding the Corrosion of Stainless Steel," Corrosion, Vol. 57, No.12, Dec. 2001, pp1030-1041.

[3] K. Ajay, S. Chaudhary and A. Sharma., "Electrochemical Studies of Stainless Steel Corrosion in Peroxide Solutions", Portugaliae Electrochimica Acta, 2012, 30(2), 99-109.

[4] J. Tian, W. Wang and M. Babar, "A New Maraging Stainless Steel with Excellent Strength–Toughness–Corrosion Synergy", Materials 2017, 10, 1293; doi:10.3390/ma10111293

[5] A. Nykiel and J. Kazior, "Effect of Aging Temperature on Corrosion Behavior of Sintered 17-4 PH Stainless Steel in Dilute Sulfuric Acid Solution", Journal of Materials Engineering and Performance (JMEPEG), Published online 15 June 2017.

[6] C. H. Beraldo, José Wilmar Calderón-Hernández, Rodrigo Magnabosco and Neusa Alonso-Falleiros, "Effect of Aging Heat Treatment H950 and H1000 on Mechanical and Pitting Corrosion Properties of UNS S46500 Stainless Steel", Materials Research. 2019; 22(1).

[7] AZO-Material, the state of scientific marketing survey, " Martensitic Stainless Steel, Applications", November 1, 2018.

[8] H. Nakagawa, T. Miyazaki and H. Yokota, "Effect of Aging Temperature on the Microstructure and Mechanical Properties of 1.8Cu-7.3Ni-15.9Cr-1.2Mo-low C, N,Martensitic Precipitation Hardening Stainless Steel," Journal of Materials and Science, 35, 2000, pp.2245-2253.

[9] P. Anja and k. Axel, "Local Corrosion of Martensitic Stainless Steels during Exposure to Saline Aquifer Water and CO2 Environment", International Journal of Chemical Engineering and Applications, Vol. 9, No. 1, February 2018.

[10] D. Deng," Microstructural Study of 17-4PH Stainless Steel after Plasma-Transferred Arc Welding", Materials 2015, 8, 424-434; doi:10.3390/ma8020424.

[11] Z. De-ning., "Influence of Tempering Process on Mechanical Properties of 00Cr13Ni4Mo Super Martensitic Stainless Steel" J. of Iron and Steel Research, International. 17(8), 2010, pp 50-54.

[12] B. Qin., "Effect of Tempering Temperature on Properties of 00Cr16Ni5Mo Stainless Steel", Materials Characterization, 59, 2008, pp 1096-1100.

دراسة تاثير التعتيق الحراري على مقاومة التآكل الكيميائي النقري للفولاذ المقاوم للصدأ المارتنسيتي

عبدالله ضايع عاصي

الجامعة التقنية الوسطى / معهد تكنولوجيا –بغداد/ العراق – بغداد

البريد الالكتروني: drabdullah_dhayea@mtu.edu.iq

الخلاصة

في هذا البحث تم دراسة تأثير المعالجة الحرارية بالتعتيق في مقاومة التآكل الكيميائي النقري للفولاذ المارتنسيتي المقاوم للصدأ، اذ عرضت عينات من الفولاذ المارتنسيتي المقاوم للصدأ إلى معالجة انحلالية عند درجة حرارة 1100 درجة مئوية مدة ساعة وغطست بالماء ومن ثم سخنت إلى درجة حرارة ضمن المجال (500-750) درجة مئوية لمدد إبقاء متنوعة (1-20) ساعة. اجري اختبار التآكل الكيميائي المسرع واختبار التآكل الكيميائي بالغمر على العينات بعد المعالجة الحرارية . بينت نتائج البحث تأثر مقاومة التآكل النقري تأثرًا كبيرًا بدرجة حرارة التعتيق، إذ وجد أن العينات المعتقة عند درجة حرارة 550 درجة مئوية تملك اعظم معدل تآكل الذي قد يكون بسبب زيادة نسبة فرايت نوع دلتا (δ-فرايت) وترسبات ناعمة جدًا من أطوار أخرى بشكل غير متجانس في الطور الأساسي المارتنسيتي؛ مما يؤدي إلى زيادة معدل التآكل، في حين العينات المعتقة في مجال درجة حرارة (550–650) درجة مئوية لها قيم معدل تآكل أصغر، ويعزى ذلك إلى النسبة الحجمية المرتفعة للأوستنيت المتبقي . وتبدي العينات المعتقة عند درجة حرارة أعلى من 650 درجة مئوية معدلَ تآكلٍ متوسطا. ووجد كذلك أن نوع النقر الناتجة عن كلا اختباري التآكل الكيميائي وشكلها لا يتعلق بشكل الفريت نوع دلتا والكربيدات الموجودة في البنية المجهرية.